

1 CYP2D6 and CYP2A6 biotransform dietary tyrosol into hydroxytyrosol

2  
3 Jose Rodríguez-Morató<sup>a,b,c</sup>, Patricia Robledo<sup>a,b</sup>, Julie-Anne Tanner<sup>d,e</sup>, Anna Boronat<sup>a,b</sup>,  
4 Clara Pérez-Mañá<sup>a,g</sup>, C-Y. Oliver Chen<sup>h</sup>, Rachel F. Tyndale<sup>d,e,f</sup> and Rafael de la  
5 Torre<sup>a,b,c,\*</sup>

6  
7 <sup>a</sup> Integrative Pharmacology and Systems Neuroscience Research Group, Neurosciences  
8 Research Program. IMIM (Hospital del Mar Medical Research Institute), Dr. Aiguader  
9 88, Barcelona 08003, Spain ([jrodriguez1@imim.es](mailto:jrodriguez1@imim.es); [probledo@imim.es](mailto:probledo@imim.es);  
10 [aboronat@imim.es](mailto:aboronat@imim.es); [cperez@imim.es](mailto:cperez@imim.es); [rtorre@imim.es](mailto:rtorre@imim.es))

11 <sup>b</sup> Department of Experimental and Health Sciences, Universitat Pompeu Fabra (CEXS-  
12 UPF), Dr. Aiguader 80, Barcelona 08003, Spain

13 <sup>c</sup> Spanish Biomedical Research Centre in Physiopathology of Obesity and Nutrition  
14 (CIBEROBN), Instituto Salud Carlos III, 28029 Madrid, Spain

15 <sup>d</sup> Campbell Family Mental Health Research Institute, Centre for Addiction and Mental  
16 Health (CAMH), Toronto, Ontario, Canada ([julianne.tanner@mail.utoronto.ca](mailto:julianne.tanner@mail.utoronto.ca))

17 <sup>e</sup> Department of Pharmacology and Toxicology, Toronto, Ontario, Canada  
18 ([r.tyndale@utoronto.ca](mailto:r.tyndale@utoronto.ca))

19 <sup>f</sup> Department of Psychiatry, Toronto, Ontario, Canada

20 <sup>g</sup> Department of Pharmacology, Therapeutics and Toxicology, Autonomous University  
21 of Barcelona, Cerdanyola, Spain

22 <sup>h</sup> Antioxidants Research Laboratory, Jean Mayer USDA Human Nutrition Research  
23 Center on Aging, Tufts University, Boston, MA 02111, United States  
24 ([Oliver.Chen@tufts.edu](mailto:Oliver.Chen@tufts.edu))

25 **\*Corresponding author:** Rafael de la Torre, PharmD, PhD. Integrative Pharmacology  
26 and Systems Neuroscience Research Group, IMIM (Hospital del Mar Medical Research  
27 Institute), Barcelona, Spain. Tel: +34 933160484; Fax: +34 933160467; E-mail:  
28 [rtorre@imim.es](mailto:rtorre@imim.es)  
29

30

## Abstract

31 The dietary phenol tyrosol has been reported to be endogenously transformed into  
32 hydroxytyrosol, a potent antioxidant with multiple health benefits. In this work, we  
33 evaluated whether tyrosine hydroxylase (TH) and cytochrome P450s (CYPs) catalyzed  
34 this process. To assess TH involvement, Wistar rats were treated with  $\alpha$ -methyl-*L*-  
35 tyrosine and tyrosol. Tyrosol was converted into hydroxytyrosol whilst  $\alpha$ -methyl-*L*-  
36 tyrosine did not inhibit the biotransformation. The role of CYP was assessed in human  
37 liver microsomes (HLM) and tyrosol-to-hydroxytyrosol conversion was observed.  
38 Screening with selective enzymatic CYP inhibitors identified CYP2A6 as the major  
39 isoform involved in this process. Studies with baculosomes further demonstrated that  
40 CYP2D6 and CYP3A4 could transform tyrosol into hydroxytyrosol. Experiments using  
41 human genotyped livers showed an interindividual variability in hydroxytyrosol  
42 formation and supported findings that CYP2D6 and CYP2A6 mediate this reaction. The  
43 dietary health benefits of tyrosol-containing foods remain to be evaluated in light of  
44 CYP pharmacogenetics.

45

46 **Keywords:** Hydroxytyrosol; tyrosol; human liver microsomes; CYP2A6; CYP2D6;  
47 metabolism.

## 48 Chemical compounds

49 Hydroxytyrosol (PubChem CID: 82755); Tyrosol (PubChem CID: 10393); Nicotine  
50 (PubChem CID: 942), Coumarin (PubChem CID: 323); Dextromethorphan (PubChem  
51 CID: 6916184); Tryptamine (PubChem CID: 1150); Methoxsalen (PubChem CID:  
52 4114); Tranlycypromine (PubChem CID: 19493).

## 53 **1. Introduction**

54 Hydroxytyrosol [HT, 2-(3,4-dihydroxyphenyl)ethanol], the main phenolic  
55 compound found in olives, virgin olive oil, and red wine, is also a product of dopamine  
56 oxidative metabolism (DOPET) (Figure 1A). The health benefits attributed to HT  
57 bioactivities include antioxidant, anti-inflammatory, cardioprotective, antitumor,  
58 antimicrobial, antidiabetic, and neuroprotective ones (Fernández-Mar, Mateos, García-  
59 Parrilla, Puertas, & Cantos-Villar, 2012; Rodríguez-Morató, Xicota, Fitó, Farré,  
60 Dierssen, & de la Torre, 2015).

61 Based on evidence that the phenolic compounds in olive oil are protective  
62 against LDL oxidation (Covas, de la Torre, & Fitó, 2015), the European Food Safety  
63 Authority (EFSA) released a claim regarding the beneficial effects of the daily ingestion  
64 of phenolic compound-rich virgin olive oil on cardiovascular disease risk factors. To  
65 achieve such benefits a daily dose of 5 mg HT and its derivatives (including tyrosol  
66 (Tyr) and oleuropein) in olive oil is required which has opened up the possibility of  
67 employing HT and Tyr as nutraceuticals.

68 The addition of a hydroxyl group at position 3 of the phenol ring provides HT  
69 with *o*-diphenol moiety, a key factor for its presenting higher antioxidant activity than  
70 Tyr (Carrasco-Pancorbo et al., 2005). Tyr content in red wine has been reported to be  
71 more than 5-fold greater than that of HT (Piñeiro, Cantos-Villar, Palma, & Puertas,  
72 2011), nevertheless, a significant amount of HT has been observed to be endogenously  
73 produced. De la Torre, Covas, Pujadas, Fitó, and Farré (2006) described that urinary HT  
74 excretion was 1.4-fold higher after the consumption of 250 mL of red wine compared to  
75 25 mL of virgin olive oil, despite the HT content being ~5-times lower (0.35 vs 1.70 mg,  
76 respectively). Moreover, urinary recovery of HT following red wine administration was  
77 greater than the amount of HT present in the wine itself, suggesting an endogenous HT

78 production. An ethanol dose-related increase of urinary HT excretion in 24 healthy men  
79 has been observed, probably through the induction of endogenous HT production  
80 (Pérez-Mañá et al., 2015). Such findings are consistent with previous work (Tank &  
81 Weiner, 1979) in which ethanol up-regulated dopamine oxidative metabolism,  
82 generating HT in a dose-dependent manner (Figure 1A).

83 Nevertheless, this ethanol-induced mechanism does not completely explain the  
84 amount of HT recovered in urine after wine intake. In a rat study it was reported that  
85 Tyr was converted *in vivo* to HT, and that Tyr urinary excretion was augmented by  
86 ethanol (Pérez-Mañá et al., 2015). Despite the fact that Tyr has been identified as a  
87 substrate of HT production, the enzyme responsible for this biotransformation remains  
88 as yet unknown. Two theoretical possibilities have been considered: the involvement of  
89 [i] tyrosine hydroxylase and/or [ii] cytochrome P450 (CYP) isoenzymes (Figure 1B).

90 Tyrosine hydroxylase is the rate-limiting enzyme in catecholamine biosynthesis  
91 and it catalyzes the aromatic hydroxylation that converts *L*-tyrosine to *L*-DOPA  
92 (Nagatsu, Levitt, & Udenfriend, 1964). Taking into account that the difference between  
93 Tyr and HT is an aromatic hydroxylation, our first hypothesis was that tyrosine  
94 hydroxylase was involved in the conversion of Tyr to HT. Alternatively, we considered  
95 CYPs which are responsible for catalyzing the oxidation of a wide variety of xenobiotic  
96 chemicals and endogenous substrates.

97 In addition to identifying the enzymes taking part in Tyr-HT biotransformation,  
98 we aimed to evaluate the effects of a combined administration of ethanol and Tyr on the  
99 urinary recovery of both Tyr and HT. To this end, the effects of the tyrosine  
100 hydroxylase inhibitor  $\alpha$ -methyl-*L*-tyrosine ( $\alpha$ MT) on this biotransformation was  
101 assessed in rats; the involvement of CYPs was examined in human liver microsomes

102 (HLM) and human recombinant proteins (baculosomes); and Tyr hydroxylation was  
103 investigated in human genotyped livers.

104

## 105 **2. Material and Methods**

### 106 **2.1. Drugs and Chemicals**

107 HT and HT acetate were supplied by Seprox Biotech (Madrid, Spain). HT-D<sub>3</sub>  
108 was purchased from Synfine Research Inc (Ontario, Canada). Tyr, 3-(4-  
109 hydroxyphenyl)-1-propanol, homovanillyl alcohol, fluvoxamine maleate, montelukast  
110 sodium hydrate, ticlopidine hydrochloride, methoxsalen, tryptamine hydrochloride,  
111 omeprazole, ketoconazole, coumarin, NADPH, sodium phosphate monobasic  
112 monohydrate, sodium phosphate dibasic anhydrous, paroxetine, fluoxetine, *o*-  
113 phosphoric acid (85%), nicotine, cotinine, cotinine-D<sub>3</sub>, coumarin, 7-hydroxycoumarin,  
114 4-hydroxycoumarin, dextromethorphan, dextrorphan, 2-benzoxazolinone, and dimethyl  
115 sulfoxide were purchased from Sigma-Aldrich Corporation (St. Louis, MO, USA).  
116 Sulfaphenazole and tranlycypromine hydrochloride were purchased from Cayman  
117 Chemical (Ann Arbor, MI, USA). HT glucuronide conjugates were synthesized  
118 according to a previously described method (Khymenets, Joglar, Clapés, Parella, Covas,  
119 & de la Torre, 2006). HT-D<sub>4</sub> was custom synthesized by Toronto Research Chemicals  
120 Inc. (Toronto, Ontario, Canada). HT-1-*O*-sulfate was custom synthesized by Industrial  
121 Research Limited (Lower Hutt, New Zealand). Methanol and acetonitrile (HPLC  
122 gradient grade), ammonium hydroxide, and acetic acid were purchased from Merck  
123 (Darmstadt, Germany). Ultrapure water was obtained using a Milli-Q purification  
124 system (Millipore Ibérica, Barcelona, Spain). Standard stock solutions of Tyr, HT, and  
125 their metabolites, as well as their corresponding internal standards (IS), were prepared  
126 using 10 mg/mL methanol. Working solutions were obtained by further diluting the  
127 stock solutions and were then stored in amber vials at -20°C.

128

### 129 **2.2. Human Liver Microsomes and Recombinant Enzymes**

130 Human liver microsomes (HLM) pooled from 50 donors were purchased from  
131 Life Technologies Europe. According to the manufacturer, total protein and P450  
132 content were 20.0 mg/mL and 0.239 nmol/mg, respectively. Microsomes produced from  
133 baculovirus-infected insect cells expressing human CYP2A6, CYP3A4, CYP2B6,  
134 CYP2C9, and CYP2D6 (Baculosomes<sup>®</sup>) were also purchased from Life Technologies  
135 Europe with the corresponding protein concentrations and CYP contents.

136 The characteristics and sources of the 15 human livers used in this study have  
137 been previously described (Messina, Tyndale, & Sellers, 1997). Human hepatic  
138 microsomes were prepared and stored in 1.15% KCl at -80°C according to previously  
139 established techniques (Tyndale, Inaba, & Kalow, 1989). Human liver tissues were  
140 derived from the K- and M-series liver banks provided by Dr. T. Inaba (University of  
141 Toronto, Toronto, ON, Canada) and Dr. U. Meyer (Biocentre in Basel, Switzerland),  
142 respectively, as previously published (Al Koudsi, Hoffmann, Assadzadeh, & Tyndale,  
143 2010; Messina, Tyndale, & Sellers, 1997). Cytosolic fractions were collected during  
144 microsomal membrane preparation and used as a source of aldehyde oxidase for all *in*  
145 *vitro* nicotine metabolism assays. Total protein was quantified with a Bio-Rad protein  
146 assay kit based on the Bradford dye-binding method (Bio-Rad Laboratories Ltd.).

147 DNA was extracted from liver tissues for CYP2A6 and CYP2D6 genotyping with  
148 phenol/chloroform extraction (Invitrogen, Canada) and ethanol precipitation. DNA was  
149 genotyped for the CYP2A6 alleles \*2, \*4, \*5, \*6, \*9, \*12, \*17, \*20, \*21, \*23, \*24, \*25,  
150 \*26, \*27, \*28, \*35, \*1X2, and the CYP2D6 alleles \*3, \*4, \*10, as previously described  
151 (Tyndale, Droll, & Sellers, 1997; Wassenaar, Zhou, & Tyndale, 2015). Liver donors  
152 were then grouped as normal or reduced CYP2A6 and CYP2D6 metabolizers based on  
153 predicted activity according to genotype. The CYP2A6 and CYP2D6 normal groups  
154 included donors of genotypes CYP2A6\*1/\*1, \*1/1X2 and CYP2D6\*1/\*1 only for each

155 gene. CYP2A6 protein levels in these human liver tissues were semi-quantified with  
156 Western blotting, as previously described (Al Koudsi, Hoffmann, Assadzadeh, &  
157 Tyndale, 2010).

158

### 159 **2.3. Animal studies**

160         Seventy-two male Wistar rats (Charles River) weighing 140-200 g were used in  
161 the experiments. They were housed two per cage (temperature  $22 \pm 2^\circ\text{C}$  / humidity  $55 \pm$   
162 15%) in a controlled room with a 12-h light/dark cycle (lights on at 08:00 h). The  
163 experiments were performed during the period of light. Food and water were given *ad*  
164 *libitum* in the home cages, but only water was available in the metabolic cages (Harvard  
165 Apparatus, 48 cm x 28 cm x 36 cm) during the four hours of the experiment. Each cage  
166 was provided with a support grid for the animals, separate urine and feces collection  
167 funnels, and a drinking tube. On the day prior to the experimental session, the rats were  
168 habituated to the metabolic cages for two hours. They were assigned to twelve  
169 treatments (N = 6/group) (Supplementary Table 1). The rats were first injected with  
170 either  $\alpha\text{MT}$  (50 mg/kg) or saline, and thirty min later received either 0.5 g/kg ethanol  
171 (30% ethanol in saline, v/v) or vehicle (saline). One hour later, they were injected with  
172 10 or 20 mg/kg of Tyr (prepared in saline) or vehicle. All treatments were administered  
173 intraperitoneally. Following the last administration, the rats were immediately placed in  
174 the cages for 4 h. and urine produced during this period collected. On terminating the  
175 experiment, the rats were euthanized under isoflurane anesthesia. Urine samples were  
176 weighed and preserved with 6N HCl (20  $\mu\text{L}/\text{mL}$  urine), and stored at  $-20^\circ\text{C}$  until  
177 analysis. HT, Tyr, and their corresponding metabolites were quantified using a LC-  
178 MS/MS method as previously described (Khymenets et al., 2010; Kotronoulas et al.,  
179 2013; Pérez-Mañá et al., 2015). Animal procedures were approved by the local ethical

180 committee (CEEA-PRBB; ref. PRM-13-1525) and performed in accordance with the  
181 guidelines of the European Communities Directive 86/609/EEC regulating animal  
182 research.

183

## 184 **2.4. Experiments in Human Liver Microsomes (HLM)**

### 185 *2.4.1. Tyrosol metabolism to hydroxytyrosol*

186 The evaluation of HT formation was carried out at 37°C in a shaking bath for 0  
187 to 60 min. The final incubation mixtures (250  $\mu$ L) contained Tyr (10 - 100  $\mu$ M), HLM  
188 (0.5 mg protein/mL), and NADPH (1 mM) in 100 mM sodium phosphate buffer (pH  
189 7.4). The reactions were initiated by the addition of the NADPH solution after a 3-min  
190 pre-incubation, and stopped at each corresponding time by the addition of 250  $\mu$ L ice-  
191 cold methanol. A negative control in the absence of NADPH was employed to verify  
192 the NADPH-dependent reaction. To each reaction mixture, 20  $\mu$ L IS solution (10  
193  $\mu$ g/mL each of HT-D<sub>3</sub> and 3-(4-hydroxyphenyl)-1-propanol) was added. The resulting  
194 mixture was centrifuged (13,000 rpm, 5 min, 4°C). The supernatant was transferred to  
195 an amber screw-top glass tube, diluted with 4.25 mL of Milli-Q water, acidified to pH 2  
196 with 250  $\mu$ L 4% H<sub>3</sub>PO<sub>4</sub>, and subjected to a solid-phase extraction (SPE) procedure  
197 (Oasis HLB<sup>®</sup> 3cc, 60-mg cartridges; Waters Corporation, Dublin, Ireland). The SPE  
198 cartridges were preconditioned sequentially with 2 mL methanol and 2 mL water. After  
199 sample loading, the cartridges were washed with 2 mL water. The compounds of  
200 interest were then eluted with 3 mL methanol. After methanol removal (25°C, 10-15  
201 psi), the dry residues were reconstituted in a 100  $\mu$ L mixture of mobile phases  
202 (90% A/10% B, v/v), centrifuged at 10,000 rpm for 3 min, transferred to HPLC vials, and  
203 analyzed by LC-MS/MS. This procedure was employed for both the mix of HLM and  
204 the individual genotyped microsomes.

205 Identification and quantification of HT and Tyr were performed using an Agilent  
206 1200 series HPLC system (Agilent technologies) coupled to a triple quadrupole (6410  
207 Triple Quad LC/MS; Agilent) mass spectrometer with an electrospray interface.  
208 Chromatographic separation of HT and Tyr was carried out on an Acquity UPLC<sup>®</sup> BEH  
209 C<sub>18</sub> column (100 mm x 3.0 mm i.d., 1.7 μm particle size) (Waters Corporation) at 40°C  
210 in an isocratic mode using 75% mobile phase A (0.01% ammonium acetate, pH 5) and  
211 25% mobile phase B (100% methanol). Injection volume was 10 μL. Tyr, HT, and the  
212 IS were eluted with the flow rate at 0.25 mL/min in 5 min and monitored in negative  
213 ionization using the multiple reaction mode. HT was quantified employing an isotope  
214 dilution method by comparing its peak area ratio with HT-D<sub>3</sub>.

#### 215 *2.4.2. Nicotine metabolism to cotinine*

216 The rates of nicotine, coumarin, and dextromethorphan metabolism were  
217 assessed *in vitro* in the HLMs from the 15 donors. The velocity of nicotine metabolism  
218 to cotinine was determined by incubating microsomal protein (0.5 mg/mL) with  
219 nicotine (30 μM), Tris-HCl buffer (pH 7.4, 50 mM), NADPH (1 mM), and 10 μL of  
220 human liver cytosol (as the aldehyde oxidase source) in the final volume of 100 μL. The  
221 reactions were carried out for 20 min at 37 °C and stopped with the addition of 20 μL of  
222 20% Na<sub>2</sub>CO<sub>3</sub>. The IS, cotinine-D<sub>3</sub>, was added. Samples were extracted and analyzed by  
223 LC-MS/MS as previously described (Tanner et al., 2015).

#### 224 *2.4.3. Coumarin metabolism to 7-hydroxycoumarin*

225 Coumarin metabolism to 7-hydroxycoumarin was evaluated by incubating  
226 microsomal protein (0.05 mg/mL) with coumarin (2 μM), Tris-HCl buffer (pH 7.4, 50  
227 mM), and NADPH (1 mM) in the final volume of 200 μL. The rate of 7-  
228 hydroxycoumarin formation was linear from 2-15 min; for fast CYP2A6 livers,  
229 according to the rate of cotinine formation from nicotine (highest tertile), shorter

230 incubation times were used to avoid substrate depletion. The reactions were carried out  
231 at 37°C and stopped with the addition of 40  $\mu\text{L}$  trichloroacetic acid (20% w/v).  
232 Following the addition of the IS, 4-hydroxycoumarin, the resulting reaction mixtures  
233 were extracted and analyzed by HPLC as previously described (Li, Li, & Sellers, 1997),  
234 with minor modifications. Briefly, after the addition of 3 mL ethyl acetate, the mixtures  
235 were vortexed for 10 seconds, mechanically shaken for 10 min, and centrifuged at 3,000  
236 rpm for 10 min. The upper ethyl acetate layer was then transferred to a 10-mL tube and  
237 evaporated to dryness at 37°C under nitrogen stream. The dry residue was re-dissolved  
238 with 110  $\mu\text{L}$  mobile phase, and 100  $\mu\text{L}$  of the solution was injected into the HPLC  
239 system (HP 1200 Separation Module). Coumarin and 7-hydroxycoumarin were  
240 separated on the ZORBAX SB C18 Column (5  $\mu\text{m}$ . 250  $\times$  4.6 mm; Agilent  
241 Technologies, Mississauga, ON) using mobile phase of acetonitrile, water and acetic  
242 acid (25:75:0.1, v/v) at 1 mL/min flow rate. The retention time of 7-hydroxycoumarin,  
243 4-hydroxycoumarin, and coumarin was 7.9, 11.8, and 17.7 min, respectively.

#### 244 *2.4.4. Dextromethorphan metabolism to dextrorphan*

245 The metabolism of dextromethorphan to dextrorphan was measured by  
246 incubating microsomal protein (0.25 mg/mL) with dextromethorphan (5  $\mu\text{M}$ ), 100 mM  
247 potassium phosphate buffer (pH 7.4), and NADPH (1 mM) in the final volume of 250  
248  $\mu\text{L}$ . The reactions were carried out for 15 min at 37°C and stopped with the addition of  
249 250  $\mu\text{L}$  hexane-butanol (95:5 v/v). The IS, 2-benzoxazolinone, was added. The resulting  
250 mixtures were extracted and analyzed by HPLC as previously described (Flores-Pérez,  
251 Flores-Pérez, Juárez-Olguín, Lares-Asseff, & Sosa-Macías, 2004; Hendrickson, Gurley,  
252 & Wessinger, 2003), with minor modifications. Specifically, 5 mL hexane-butanol  
253 (95:5 v/v) was first added, and the same procedure used for coumarin (see subheading  
254 2.4.2.) was followed. Separation of dextromethorphan and dextrorphan was carried out

255 with a ZORBAX Bonus-RP column (5  $\mu\text{m}$ , 250 $\times$ 4.6 mm; Agilent Technologies,  
256 Mississauga, ON) under a gradient elution condition using solvent A (methanol and  
257 0.05 M phosphate buffer, 45:55 v/v, pH 5.8) and solvent B (water) at room temperature.  
258 The linear gradient from 100% to 70% solvent A was applied from 0 to 14 min at a flow  
259 rate of 0.8 mL/min. From 14 to 27 min, the mobile phase was kept constant at 100%  
260 solvent A and 1.2 mL/min flow rate. The eluents were monitored by a fluorescence  
261 detector set at an excitation/emission wavelength of 230/330 nm. Retention time was  
262 10.52, 13.26, and 22.63 min for dextrorphan, 2-benzoxazolinone, and dextromethorphan,  
263 respectively.

264

## 265 **2.5. Enzyme Kinetics Experiments**

266 Tyr, at concentrations ranging from 0.1 to 4000  $\mu\text{M}$ , was incubated with HLM  
267 and the procedure described in the subheading 2.4.1. was followed. All kinetic analyses  
268 were performed in duplicate. The kinetic parameters ( $K_m$  and  $V_{max}$ ) were estimated  
269 using the Michaelis-Menten equation generated by GraphPad Prism (GraphPad  
270 Software, CA, USA, version 5.03 for Windows).

271 Tyr was also incubated in CYP2A6 and CYP2D6 baculosomes for 60 and 15  
272 min, respectively. These time-points were chosen based on preliminary experiments  
273 evaluating enzymatic reaction linearity (Supplementary Figure 1). The curves  
274 describing the reaction kinetics were analyzed using non-linear regression analysis  
275 (GraphPad Software 5.03, CA, USA).

276

## 277 **2.6. Chemical Inhibition Analyses**

278 The effects of specific CYP inhibitors on tyrosol hydroxylase activity in HLM  
279 were investigated. Tyr (final concentration of 100  $\mu\text{M}$ ) was incubated with pooled HLM

280 (0.5 mg/mL) and NADPH (1 mM) in the absence (positive control) and presence of  
281 selective chemical inhibitors of CYP isoforms. All the chemical inhibition studies were  
282 performed in duplicate. The following CYP inhibitors were used: fluvoxamine for  
283 CYP1A2, ticlopidine for CYP2B6, montelukast for CYP2C8, sulfaphenazole for  
284 CYP2C9, omeprazole for CYP2C19, quinidine for CYP2D6, and ketoconazole for  
285 CYP3A4. In the case of CYP2A6, the substrate coumarin was employed (See  
286 Supplementary Figure 2 for the chemical structures). The specific inhibitors were  
287 chosen following the European Medicine Agency guidelines on the Investigation of  
288 Drug Interactions (EMA, 2012). The following additional inhibitors were also used in  
289 confirmatory experiments with tryptamine, tranylecypromine, and methoxsalen as  
290 CYP2A6 inhibitors, and paroxetine and fluoxetine as CYP2D6 inhibitors. The range of  
291 inhibitor concentrations was 1-100  $\mu$ M. Initially, stock solutions of CYP inhibitors were  
292 prepared in DMSO. The final DMSO concentration in the reactions was 1.0%. Due to a  
293 remarked DMSO-induced inhibitory effect on the reaction, working inhibitor solutions  
294 were prepared in methanol. In order to avoid any interference from organic solvent, the  
295 inhibitors were prepared in methanol to facilitate solvent removal for the assay.  
296 Methanol was evaporated in a vacuum concentrator (SpeedVac<sup>®</sup>). The reaction mixture  
297 excluding NADPH was added to tubes containing inhibitors. The reactions were started  
298 by the addition of NADPH and were stopped at 60 min by the addition of 250  $\mu$ L ice-  
299 cold methanol.

300 Additional inhibitory experiments were performed to assess the effect of  
301 mechanism-based inhibitors (methoxsalen for CYP2A6, paroxetine for CYP2D6) on  
302 HT formation. In these cases, the inhibitor was pre-incubated with microsomes and  
303 NADPH for 30 min prior to the addition of the substrate. The reaction mixture was then  
304 incubated at 37°C for another 30 min, and treated as previously described.

305

## 306 **2.7. HT formation in cDNA-Expressing CYP microsomes**

307 Incubations were carried out at 37°C in a shaking bath for 0 to 60 min. The final  
308 incubation mixtures (250 µL) contained Tyr (40-400 µM), the corresponding cDNA-  
309 expressing CYP microsomes (40-80 pmol CYP/mL), and NADPH (1 mM) in 100 mM  
310 sodium phosphate buffer (pH 7.4). The reactions were started by the addition of  
311 NADPH solution after a 3-min pre-incubation and stopped at selected times (0-60 min)  
312 by the addition of 250 µL ice-cold methanol. A negative control in the absence of  
313 NADPH was employed to verify the NADPH-dependent reaction. Prior to analysis, the  
314 samples were processed as described for HLM samples.

315

## 316 **2.8. Statistical Analyses**

317 Data analyses of animal and chemical inhibition studies were performed using  
318 a three-way ANOVA model (to evaluate effects of Tyr, ethanol, and αMT on HT  
319 urinary excretion) as well as a two-way ANOVA (to assess the effects of Tyr and  
320 ethanol on Tyr urinary excretion). *Post hoc* multiple comparisons were performed for  
321 statistically significant results in the global analyses with the LSD test. The correlations  
322 between (1) HT formation from Tyr, and 7-hydroxycoumarin formation from coumarin,  
323 and (2) HT formation from Tyr, and dextrorphan formation from dextromethorphan  
324 were determined by Spearman's coefficient. Associations between HT production and  
325 *CYP2A6* genotype and *CYP2D6* genotype were analysed with the Mann-Whitney test.  
326 Statistical analyses were performed using SPSS Statistics for Windows (Version 21.0;  
327 SPSS Inc. Chicago, IL, USA). The level of statistical significance was defined as *P*  
328 <0.05. The results in rats are expressed as mean ± S.E.M., and the *in vitro* findings as  
329 mean ± S.D.

330           Data mining for Tyr-to-HT conversion in individual genotyped livers, multiple  
331 regression analysis, and 3D graphics were performed with MATLAB software version  
332 7.0. Experimental data were fitted to a quadratic equation including two linear terms  
333 and a quadratic one in order to obtain the optimum correlation.  
334

### 335 **3. Results**

#### 336 **3.1. Animal experiments**

337 A dose-dependent increase in total Tyr urinary recovery was found following  
338 Tyr administration (Figure 2A). A two-way ANOVA revealed a main effect of Tyr  
339 ( $F_{(2,28)} = 92.2$ ,  $p < 0.001$ ) although no significant effect of ethanol or interaction between  
340 factors were observed, indicating that ethanol does not modify the excretion of Tyr  
341 (Figure 2A).

342 A three-way ANOVA evaluating the action of Tyr, ethanol, and  $\alpha$ MT on total  
343 HT urinary recovery showed a main effect of Tyr ( $F_{(2,42)} = 23.7$ ,  $p < 0.001$ ) and ethanol  
344 ( $F_{(1,42)} = 11.1$ ,  $p < 0.001$ ), but none of  $\alpha$ MT. No interactions amongst factors were  
345 observed. However, the results in Figure 2B demonstrate that Tyr increased total  
346 urinary HT recovery in a dose-dependent fashion, while  $\alpha$ MT did not significantly  
347 inhibit this effect at the dose studied. Ethanol slightly inhibited the conversion of Tyr to  
348 HT without reaching statistical significance. The combination of  $\alpha$ MT and ethanol also  
349 decreased HT formation although this effect was mainly due to the inhibitory action of  
350 ethanol (Figure 2B).

351

#### 352 **3.2. Tyrosol hydroxylase activity in HLM**

353 HT formation from Tyr took place in human hepatic microsomes in an NADPH-  
354 dependent manner and increased in a linear fashion ( $r^2 > 0.98$ ) from 0 to 60 min reaction  
355 time. This hydroxylation activity occurred in a substrate concentration-dependent  
356 manner (Figure 3A).

357

#### 358 **3.3. Kinetic analyses of Tyrosol *ortho*-hydroxylation in HLM**

359 Figure 3 shows the Michaelis-Menten, Lineweaver-Burk, and Eadie-Hofstee  
360 plots for the HLM-mediated HT formation from Tyr. The values represent the mean of  
361 two separate experiments. The apparent  $K_m$  value was  $709 \pm 49 \mu\text{M}$  and the  $V_{\text{max}}$  value  
362 was  $1294 \pm 31 \text{ pmol/min/mg}$ .

363

#### 364 **3.4. Chemical inhibition studies with specific CYP inhibitors**

365 The effect of 8 CYP inhibitors on HT formation from Tyr was evaluated. Firstly,  
366 a primary screening using 8 specific inhibitors at  $100 \mu\text{M}$  was performed. Figure 4  
367 shows the mean activities (from duplicate determinations) in the presence of these  
368 inhibitors. Coumarin reduced HT formation from Tyr ( $100 \mu\text{M}$ ) by 60%. CYP2D6,  
369 CYP3A4, CYP2B6, and CYP2C9 selective inhibitors slightly diminished HT formation  
370 ( $>10\%$  but  $< 20\%$ ) (Figure 4A).

371 Additional incubations using nicotine as a CYP2A6 substrate and tryptamine,  
372 methoxsalen, and tranlycypromine as CYP2A6 inhibitors (Zhang, Kilicarslan, Tyndale,  
373 & Sellers, 2001) were performed. Although nicotine was not found to decrease HT  
374 formation, three CYP2A6 inhibitors reduced the biotransformation to a larger degree  
375 than coumarin (74%, 77%, and 85%, respectively), with tranlycypromine being the  
376 strongest (Figure 4B). It is worth noting that the rate of coumarin metabolism by  
377 CYP2A6 is relatively fast compared to the other substrates/inhibitors tested.

378 Several inhibitors of CYP2D6 (quinidine, fluoxetine, paroxetine) and CYP2A6  
379 (tranlycypromine, methoxsalen) were pre-incubated with NADPH and microsomes for  
380 30 min and, after the addition of Tyr, the reactions took place for 30 additional min.  
381 Pre-incubation with the CYP2D6 inhibitors did not lead to a  $>20\%$  inhibition, whereas  
382 the CYP2A6 inhibitors surpassed 90%. It is of interest that the combination of two  
383 mechanism-based inhibitors, paroxetine (CYP2D6) and methoxsalen (CYP2A6),

384 inhibited HT formation by 97% (Figure 4C). No inhibitory effect was observed when a  
385 deuterated analog of HT (HT-D<sub>4</sub>) was added at 1, 10, and 100 μM to the reaction  
386 mixture, indicating there was no product-initiated inhibition of the reaction.

387

### 388 **3.5. Experiments using human recombinant CYP enzymes (Baculosomes)**

389 HT formation from Tyr was evaluated in baculosomes (microsomes from  
390 baculovirus-infected insect cells expressing human isoforms). CYP2A6 capacity for  
391 hydroxylating tyrosol was confirmed, and HT was found to be produced in a linear  
392 fashion ( $r^2 > 0.99$ ) with the amount of administered protein and Tyr (Supplementary  
393 Figure 3).

394 In order to evaluate whether other CYP isoforms could contribute to HT  
395 production, human recombinant CYP3A4, CYP2B6, CYP2C9, and CYP2D6 (as well as  
396 CYP2A6) were tested. These isoforms were chosen based on the results of the chemical  
397 inhibition assays (Figure 4A) in which the treatment with specific inhibitors of these  
398 isoenzymes decreased by HT formation by at least 10%. All the five human  
399 recombinant CYP isoforms evaluated were capable of transforming Tyr into HT with  
400 CYP2D6, CYP3A4, and CYP2A6 being more reactive than CYP2B6 and CYP2C9  
401 (Supplementary Figure 4). In all the cases, HT formation was NADPH-dependent.

402 The enzyme kinetics of CYP2D6, CYP3A4, and CYP2A6 (the 3 major  
403 contributors) were evaluated individually at 6 time points (0, 5, 15, 30, 45, and 60 min).  
404 Differing kinetics were noted for each enzyme. CYP2A6-mediated HT formation  
405 occurred in a linear time-dependent manner from 0 to 60 min. The linearity in HT  
406 formation mediated by CYP3A4 and CYP2D6 was observed only in the first 15 min,  
407 and there was a time-dependent reduction in HT content from 15 to 60 min  
408 (Supplementary Figure 1).

409 The relationship between Tyr concentration and HT formation rate was  
410 evaluated in CYP2A6 and CYP2D6 baculosomes with the aim of comparing their  
411 kinetic parameters with those obtained using HLM. HT formation kinetics in  
412 baculosomes did not follow a typical Michaelis-Menten hyperbolic pattern. In the case  
413 of CYP2A6, a biphasic kinetic profile was observed (Supplementary Figure 5A). This  
414 enzymatic behavior has been previously described (Hutzler & Tracy, 2002) and is  
415 characterized as a non-asymptotic profile that becomes linear with increasing substrate  
416 concentration. With respect to CYP2D6, the kinetics followed a sigmoidal  
417 autoactivation profile (Supplementary Figure 5B).

418

### 419 **3.6. Correlation of Tyr Hydroxylation by Individual HLM**

420 HT formation from Tyr was evaluated in 15 individual genotyped livers, which  
421 exhibited a wide range of CYP2D6 and CYP2A6 activities. Table 1 shows the  
422 individual genotypes for CYP2D6 and CYP2A6 and the predicted activities of both  
423 isoforms according to genotype.

424 The correlation between HT formation and CYP2A6 and CYP2D6 activities  
425 (determined using the metabolism velocity of coumarin to 7-hydroxycoumarin, and  
426 dextromethorphan to dextrorphan, respectively) was non-significant (Figure 5A and B).  
427 The impact of genotype on the association between HT formation and *CYP2A6* and  
428 *CYP2D6* genotypes was non-significant (Figure 5C and D).

429 In order to evaluate the concomitant involvement of both isoforms on HT  
430 formation, we performed a multivariate regression analysis. A three-dimensional scatter  
431 plot for the sample-to-sample variation in Tyr hydroxylation of the 15 individual HLMs,  
432 and their correlations with the individual CYP2D6 and CYP2A6 activities, is depicted

433 in Figure 5E. The equation of the adjusted surface that describes the velocity of Tyr  
434 hydroxylation is:

$$435 \quad \text{Tyr hydroxylation} = 0.01263 + 0.52778 \cdot X_1 + 0.044483 \cdot X_2 - 0.57453 \cdot X_1 \cdot X_2$$

436 Where  $X_1$  is dextromethorphan velocity and  $X_2$  is coumarin velocity. The  
437 corresponding correlation coefficient ( $r^2$ ) is 0.50 ( $F = 3.69$ ;  $P = 0.047$ ). It should be  
438 noted that the regression coefficient values were comparable when CYP2A6 velocity  
439 toward either coumarin or nicotine was included in the analysis.

440

#### 441 **4. Discussion**

442 Recent studies have demonstrated that HT is endogenously formed from Tyr in  
443 both rats and humans (Pérez-Mañá et al., 2015). However, the enzymes that mediated  
444 the conversion remained to be characterized. To the best of our knowledge, we  
445 demonstrate for the first time that CYPs convert Tyr into HT, and that this reaction is  
446 primarily mediated by two polymorphic CYP isoenzymes, CYP2D6 and CYP2A6.  
447 Furthermore, we observed that tyrosine hydroxylase was not involved in the conversion.

448 We hypothesized that the conversion of Tyr to HT was mediated by either  
449 tyrosine hydroxylase or CYPs. In order to examine the possible role of tyrosine  
450 hydroxylase in the formation of HT from Tyr, rates were pretreated with  $\alpha$ MT, a  
451 tyrosine hydroxylase inhibitor, before Tyr administration. The unchanged urinary HT  
452 excretion provided strong evidence that tyrosine hydroxylase was not involved in the  
453 conversion of Tyr to HT. In the same rat study, it was confirmed that urinary HT  
454 excretion occurred in parallel to the administered Tyr doses, while 0.5 g/kg ethanol  
455 slightly inhibited this effect. It is noteworthy that ethanol plays a dual role: it alters  
456 dopamine oxidative metabolism generating small amounts of HT, whilst appearing to  
457 inhibit the conversion of Tyr into HT.

458           Having demonstrated that tyrosine hydroxylase was not involved in HT  
459 formation, we next tested whether CYPs were capable of mediating Tyr hydroxylation.  
460 *In vitro* HLM experiments confirmed that at least one CYP isoform took part in the  
461 conversion of Tyr to HT via hydroxylation with a typical Michaelis-Menten kinetic  
462 profile. Such a combination of high  $K_m$  and  $V_{max}$  values indicates that, despite  
463 presenting a low specificity, Tyr-3-hydroxylation occurs at a high velocity.

464           Once Tyr hydroxylation had been demonstrated to occur in human microsomes,  
465 it was necessary to identify the specific CYP isoenzyme(s) that catalyze(s) the reaction.  
466 Results from the HLM experiments using selective inhibitors suggested that CYP2A6  
467 was the main isoform responsible for the conversion of Tyr to HT, although CYP2D6  
468 and CYP3A4 appeared to be involved to a lesser extent. The use of baculosomes  
469 (recombinant baculovirus containing cDNA) confirmed the capacity of CYP2A6,  
470 CYP2D6, and CYP3A4 to biotransform Tyr to HT.

471           The involvement of CYP3A4 baculosomes in the conversion of Tyr to HT is not  
472 surprising as it is the most abundant isoform in the liver, and it metabolizes the greatest  
473 number of drugs and other xenobiotics (Pelkonen, Turpeinen, Hakkola, Honkakoski,  
474 Hukkanen, & Raunio, 2008). Nevertheless, according to inhibition experiments with  
475 ketoconazole in pooled human liver microsomes, it should be noted that CYP3A4 is not  
476 a strong contributor to *in vivo* HT formation. The role of CYP2A6 and CYP2D6 in the  
477 conversion of Tyr to HT appears to be of greater relevance. Findings from HLM  
478 experiments using methoxsalen and paroxetine, two mechanism-based inhibitors of  
479 CYP2A6 and CYP2D6, respectively, suggest that both isoforms react toward Tyr in a  
480 cooperative manner with CYP2A6 as the major contributor and CYP2D6 the minor one.  
481 The kinetics of HT formation mediated by CYP2A6 and CYP2D6 was evaluated in  
482 baculosomes. Contrary to what occurred in microsomes, HT formation in baculosomes

483 did not follow the typical hyperbolic Michaelis-Menten kinetic profile. CYP2A6  
484 presented a biphasic kinetic profile without saturation, even at high concentrations,  
485 whilst CYP2D6 had a sigmoidal autoactivation one. Such atypical kinetic profiles have  
486 been previously described *in vitro*, especially for CYP3A4 (Hutzler & Tracy, 2002),  
487 suggesting that they might result from the simultaneous binding of multiple ligands to a  
488 single active site (Atkins, 2005). In our study, the lack of Michaelis-Menten kinetic  
489 profiles in baculosomes hindered the comparison of the individual contributions of  
490 CYP2A6 and CYP2D6 to HT formation, although at equimolar concentration CYP2D6  
491 presented a higher velocity of HT formation than CYP2A6. The discrepancy between  
492 the kinetic profile observed in microsomes and baculosomes may be due to the fact that  
493 recombinant CYP enzymes are usually expressed with much higher levels of NADPH  
494 and CYP reductase than those found in HLMs (Rodrigues, 2008). Moreover, Tyr  
495 hydroxylation in a mix of 50 HLMs (presenting a more physiological condition than  
496 baculosomes) fully coincided with a typical Michaelis-Menten kinetic profile. Taking  
497 into account the previous observations, we suggest that *in vivo* Tyr hydroxylation  
498 follows a Michaelis-Menten kinetic profile.

499         There is high interindividual variability in CYP2A6 and CYP2D6 activities due  
500 to genetic polymorphisms (Yokoi & Kamataki, 1998). CYP2D6, which catalyzes more  
501 than 25% of commercial drugs, has a gene locus with more than 80 allelic variants,  
502 resulting in considerable differences associated with increased or reduced enzymatic  
503 activity and clinical consequences (Teh & Bertilsson, 2012). In a similar manner, the  
504 *CYP2A6* gene is polymorphic, resulting in high interindividual (Rautio, Kraul, Kojo,  
505 Salmela, & Pelkonen, 1992) and interethnic divergence in enzyme activity (Piliguian et  
506 al., 2014; Raunio, Rautio, Gullsten, & Pelkonen, 2001). Indeed, 20% of Asians are  
507 *CYP2A6* poor metabolizers, whereas this prevalence is lower in Caucasians (< 1%)

508 (Raunio, Rautio, Gullsten, & Pelkonen, 2001). Regarding the relative abundance of  
509 protein in the liver, CYP2D6 accounts for less than 5% whilst CYP2A6 represents  
510 approximately 10% of total hepatic CYP protein (Pelkonen, Turpeinen, Hakkola,  
511 Honkakoski, Hukkanen, & Raunio, 2008).

512 The specificity of each CYP isoform toward its substrates is another issue that  
513 must be taken into account. CYP2D6 and CYP3A4 are responsible for the metabolism  
514 of hundreds of therapeutic drugs (Pelkonen, Turpeinen, Hakkola, Honkakoski,  
515 Hukkanen, & Raunio, 2008) whilst relatively few are converted by CYP2A6, the  
516 enzyme primarily responsible for nicotine metabolism (Messina, Tyndale, & Sellers,  
517 1997).

518 In this study, CYP2A6 and CYP2D6 from the 15 selected livers were classified  
519 according to genotype-predicted activities, and their capacity for nicotine-to-cotinine  
520 conversion and dextromethorphan-to-dextrorphan conversion, respectively. As expected,  
521 a wide interindividual Tyr-to-HT conversion variability was found. It was also observed  
522 that the correlations between HT formation and coumarin (a CYP2A6 substrate) and  
523 dextromethorphan (a CYP2D6 substrate) velocity were weak (Spearman  $r = 0.28$  in  
524 both cases) although there were modest associations between HT formation and  
525 CYP2A6/CYP2D6 activities. These results, and the previous findings with respect to  
526 baculosomes (reporting the involvement of CYP2D6 and CYP2A6) and inhibition  
527 studies with microsomes (demonstrating CYP2A6 function), indicate that both CYP2D6  
528 and CYP2A6 are actively involved in HT formation from Tyr. An implication that is  
529 further upheld by the larger regression coefficient generated in the multivariate  
530 regression analysis with CYP2D6 and CYP2A6 velocities as two independent variables.

531 Our study has strengths and limitations. One strength is the combination of *in*  
532 *vivo* (animal models) and *in vitro* (microsomes and baculosomes) techniques employed,

533 as well as the use of human livers. A limitation is the relatively low number of human  
534 livers used due to the difficulty in obtaining these samples.

535

## 536 **5. Conclusions**

537 In conclusion, our study demonstrates for the first time that HT (a potent  
538 bioactive molecule with multiple health benefits) is formed from dietary Tyr in HLMs  
539 via CYP2A6 and CYP2D6, both working in a cooperative manner. The involvement of  
540 two CYP isoenzymes in the production of HT is relevant since to date only a few  
541 known substrates of CYP2A6 have been reported. Moreover, the genetic  
542 polymorphisms of both *CYP2D6* and *CYP2A6* could have a potential impact on the  
543 magnitude of health benefits associated with the consumption of Tyr-containing food  
544 amongst individuals and ethnicities.

545

546           **Conflict of interest**

547           RFT has consulted for Apotex on unrelated issues. The other authors declare that  
548 they have no conflict of interest.

549           **Acknowledgements**

550           The authors gratefully acknowledge the assistance of Professor J. Casabó  
551 (Universitat Autònoma de Barcelona) in performing data mining, multiple regression  
552 analysis, and 3D graphics.

553           This work was supported by grants from Instituto de Salud Carlos III FEDER,  
554 (PI14/00072), the CICYT-FEDER (AGL2009-13517-C03-01 and AGL2012-40144-  
555 C03-01), grants from DIUE of the Generalitat de Catalunya (2014 SGR 680). CIBER de  
556 Fisiopatología de la Obesidad y Nutrición (CIBEROBN) is an initiative of the Instituto  
557 de Salud Carlos III, Madrid, Spain. JRM was supported by a FI-DGR2012 predoctoral  
558 fellowship from the Generalitat de Catalunya and CPM was supported by a Juan Rodés  
559 fellowship (ISCIII, JR, 15/00005). The authors acknowledge the support received from  
560 National Institutes of Health grant DA U01 020830, Canadian Institutes of Health  
561 Research grant MOP86471, the Endowed Chair in Addiction for the Department of  
562 Psychiatry University of Toronto (RFT), and funds from the Centre for Addiction and  
563 Mental Health (CAMH) and the CAMH Foundation (RFT).

564

565

## References

566 Al Koudsi, N., Hoffmann, E., Assadzadeh, A., & Tyndale, R. (2010). Hepatic CYP2A6  
567 levels and nicotine metabolism: impact of genetic, physiological, environmental,  
568 and epigenetic factors. *European Journal of Clinical Pharmacology*, 66 (3),  
569 239-251.

570 Atkins, W. M. (2005). Non-Michaelis-Menten Kinetics in Cytochrome P450-Catalyzed  
571 Reactions. *Annual Review of Pharmacology and Toxicology*, 45 (1), 291-310.

572 Carrasco-Pancorbo, A., Cerretani, L., Bendini, A., Segura-Carretero, A., Del Carlo, M.,  
573 Gallina-Toschi, T., Lercker, G., Compagnone, D., & Fernández-Gutiérrez, A.  
574 (2005). Evaluation of the Antioxidant Capacity of Individual Phenolic  
575 Compounds in Virgin Olive Oil. *Journal of Agricultural and Food Chemistry*,  
576 53 (23), 8918-8925.

577 Covas, M.-I., de la Torre, R., & Fitó, M. (2015). Virgin olive oil: a key food for  
578 cardiovascular risk protection. *British Journal of Nutrition*, 113 (SupplementS2),  
579 S19-S28.

580 De la Torre, R., Covas, M. I., Pujadas, M. A., Fitó, M., & Farré, M. (2006). Is dopamine  
581 behind the health benefits of red wine? *European Journal of Nutrition*, 45 (5),  
582 307-310.

583 EFSA. Panel on Dietetic Products, Nutrition and Allergies (NDA); Scientific Opinion  
584 on the substantiation of health claims related to polyphenols in olive and  
585 protection of LDL particles from oxidative damage (ID 1333, 1638, 1639, 1696,  
586 2865), maintenance of normal blood HDL-cholesterol concentrations (ID 1639),  
587 maintenance of normal blood pressure (ID 3781), “anti-inflammatory properties”  
588 (ID 1882), “contributes to the upper respiratory tract health” (ID 3468), “can  
589 help to maintain a normal function of gastrointestinal tract” (3779), and

590 “contributes to body defences against external agents” (ID 3467) pursuant to  
591 Article 13 (1) of Regulation (EC) No 1924/2006. EFSA J. 2011, 9, 2033,  
592 doi:10.2903/j.efsa.2011.2033. Available online:  
593 <http://www.efsa.europa.eu/efsajournal> (accessed on 12 March 2015).

594 European Medicines Agency. (2012). URL:  
595 [http://www.ema.europa.eu/docs/en\\_GB/document\\_library/Scientific\\_guideline/2](http://www.ema.europa.eu/docs/en_GB/document_library/Scientific_guideline/2012/07/WC500129606.pdf)  
596 [012/07/WC500129606.pdf](http://www.ema.europa.eu/docs/en_GB/document_library/Scientific_guideline/2012/07/WC500129606.pdf) Accessed 17.11.2014.

597 Fernández-Mar, M. I., Mateos, R., García-Parrilla, M. C., Puertas, B., & Cantos-Villar,  
598 E. (2012). Bioactive compounds in wine: Resveratrol, hydroxytyrosol and  
599 melatonin: A review. *Food Chemistry*, 130 (4), 797-813.

600 Flores-Pérez, J., Flores-Pérez, C., Juárez-Olguín, H., Lares-Asseff, I., & Sosa-Macías,  
601 M. (2004). Determination of Dextromethorphan and Dextrorphan in Human  
602 Urine by High Performance Liquid Chromatography for Pharmacogenetic  
603 Investigations. *Chromatographia*, 59 (7-8), 481-485.

604 Hendrickson, H. P., Gurley, B. J., & Wessinger, W. D. (2003). Determination of  
605 dextromethorphan and its metabolites in rat serum by liquid-liquid extraction  
606 and liquid chromatography with fluorescence detection. *Journal of*  
607 *Chromatography B*, 788 (2), 261-268.

608 Hutzler, J. M., & Tracy, T. S. (2002). Atypical Kinetic Profiles in Drug Metabolism  
609 Reactions. *Drug Metabolism and Disposition*, 30 (4), 355-362.

610 Khymenets, O., Fitó, M., Touriño, S., Muñoz-Aguayo, D., Pujadas, M., Torres, J. L.,  
611 Joglar, J., Farré, M., Covas, M.-I., & de la Torre, R. (2010). Antioxidant  
612 Activities of Hydroxytyrosol Main Metabolites Do Not Contribute to Beneficial  
613 Health Effects after Olive Oil Ingestion. *Drug Metabolism and Disposition*, 38  
614 (9), 1417-1421.

615 Khymenets, O., Joglar, J., Clapés, P., Parella, T., Covas, M.-I., & de la Torre, R. (2006).  
616 Biocatalyzed Synthesis and Structural Characterization of Monoglucuronides of  
617 Hydroxytyrosol, Tyrosol, Homovanillic Alcohol, and 3-(4'-  
618 Hydroxyphenyl)propanol. *Advanced Synthesis & Catalysis*, 348 (15), 2155-2162.

619 Kotronoulas, A., Pizarro, N., Serra, A., Robledo, P., Joglar, J., Rubió, L., Hernaéz, Á.,  
620 Tormos, C., Motilva, M. J., Fitó, M., Covas, M.-I., Solà, R., Farré, M., Saez, G.,  
621 & de la Torre, R. (2013). Dose-dependent metabolic disposition of  
622 hydroxytyrosol and formation of mercapturates in rats. *Pharmacological*  
623 *Research*, 77, 47-56.

624 Li, Y., Li, N. Y., & Sellers, E. M. (1997). Comparison of CYP2A6 catalytic activity on  
625 coumarin 7-hydroxylation in human and monkey liver microsomes. *European*  
626 *Journal of Drug Metabolism and Pharmacokinetics*, 22 (4), 295-304.

627 Messina, E. S., Tyndale, R. F., & Sellers, E. M. (1997). A Major Role for CYP2A6 in  
628 Nicotine C-Oxidation by Human Liver Microsomes. *Journal of Pharmacology*  
629 *and Experimental Therapeutics*, 282 (3), 1608-1614.

630 Nagatsu, T., Levitt, M., & Udenfriend, S. (1964). Tyrosine Hydroxylase. The Initial  
631 Step in Norepinephrine Biosynthesis. *Journal of Biological Chemistry*, 239,  
632 2910-2917.

633 Pelkonen, O., Turpeinen, M., Hakkola, J., Honkakoski, P., Hukkanen, J., & Raunio, H.  
634 (2008). Inhibition and induction of human cytochrome P450 enzymes: current  
635 status. *Archives of Toxicology*, 82 (10), 667-715.

636 Pérez-Mañá, C., Farre, M., Pujadas, M., Mustata, C., Menoyo, E., Pastor, A., Langohr,  
637 K., & de la Torre, R. (2015). Ethanol induces hydroxytyrosol formation in  
638 humans. *Pharmacological Research*, 95-96, 27-33.

639 Pérez-Mañá, C., Farré, M., Rodríguez-Morató, J., Papaseit, E., Pujadas, M., Fitó, M.,  
640 Robledo, P., Covas, M. I., Cheynier, V., Meudec, E., Escudier, J. L., & de la  
641 Torre, R. (2015). Moderate consumption of wine, through both its phenolic  
642 compounds and alcohol content, promotes hydroxytyrosol endogenous  
643 generation in humans. A randomized controlled trial. *Molecular Nutrition &*  
644 *Food Research*, 59 (6), 1213-1216.

645 Piliguián, M., Zhu, A. Z. X., Zhou, Q., Benowitz, N. L., Ahluwalia, J. S., Cox, L. S., &  
646 Tyndale, R. F. (2014). Novel CYP2A6 variants identified in African Americans  
647 are associated with slow nicotine metabolism in vitro and in vivo.  
648 *Pharmacogenetics and Genomics*, 24 (2), 118-128.

649 Piñeiro, Z., Cantos-Villar, E., Palma, M., & Puertas, B. (2011). Direct Liquid  
650 Chromatography Method for the Simultaneous Quantification of Hydroxytyrosol  
651 and Tyrosol in Red Wines. *Journal of Agricultural and Food Chemistry*, 59 (21),  
652 11683-11689.

653 Raunio, H., Rautio, A., Gullsten, H., & Pelkonen, O. (2001). Polymorphisms of  
654 CYP2A6 and its practical consequences. *British Journal of Clinical*  
655 *Pharmacology*, 52 (4), 357-363.

656 Rautio, A., Kraul, H., Kojo, A., Salmela, E., & Pelkonen, O. (1992). Interindividual  
657 variability of coumarin 7-hydroxylation in healthy volunteers.  
658 *Pharmacogenetics*, 2 (5), 227-233.

659 Rodrigues, A. D. (2008). *In Vitro* Approaches for Studying the Inhibition of Drug-  
660 Metabolizing Enzymes and Identifying the Drug-Metabolizing Enzymes  
661 Responsible for the Metabolism of Drugs (Reaction Phenotyping) with Emphasis on  
662 Cytochrome P450. *Drug-Drug Interactions*, Chapter 7, 332-334. Rodríguez-Morató,  
663 J., Xicota, L., Fitó, M., Farré, M., Dierssen, M., & de la Torre, R. (2015).

664 Potential Role of Olive Oil Phenolic Compounds in the Prevention of  
665 Neurodegenerative Diseases. *Molecules*, 20 (3), 4655-4680.

666 Tank, A. W., & Weiner, H. (1979). Ethanol-induced alteration of dopamine metabolism  
667 in rat liver. *Biochemical Pharmacology*, 28 (20), 3139-3147.

668 Tanner, J. A., Novalen, M., Jatlow, P., Huestis, M. A., Murphy, S. E., Kaprio, J.,  
669 Kankaanpaa, A., Galanti, L., Stefan, C., George, T. P., Benowitz, N. L., Lerman,  
670 C., & Tyndale, R. F. (2015). Nicotine metabolite ratio (3-  
671 hydroxycotinine/cotinine) in plasma and urine by different analytical methods  
672 and laboratories: implications for clinical implementation. *Cancer Epidemiology,*  
673 *Biomarkers & Prevention*, 24 (8), 1239-1246.

674 Teh, L. K., & Bertilsson, L. (2012). Pharmacogenomics of CYP2D6: molecular genetics,  
675 interethnic differences and clinical importance. *Drug Metabolism and*  
676 *Pharmacokinetics*, 27 (1), 55-67.

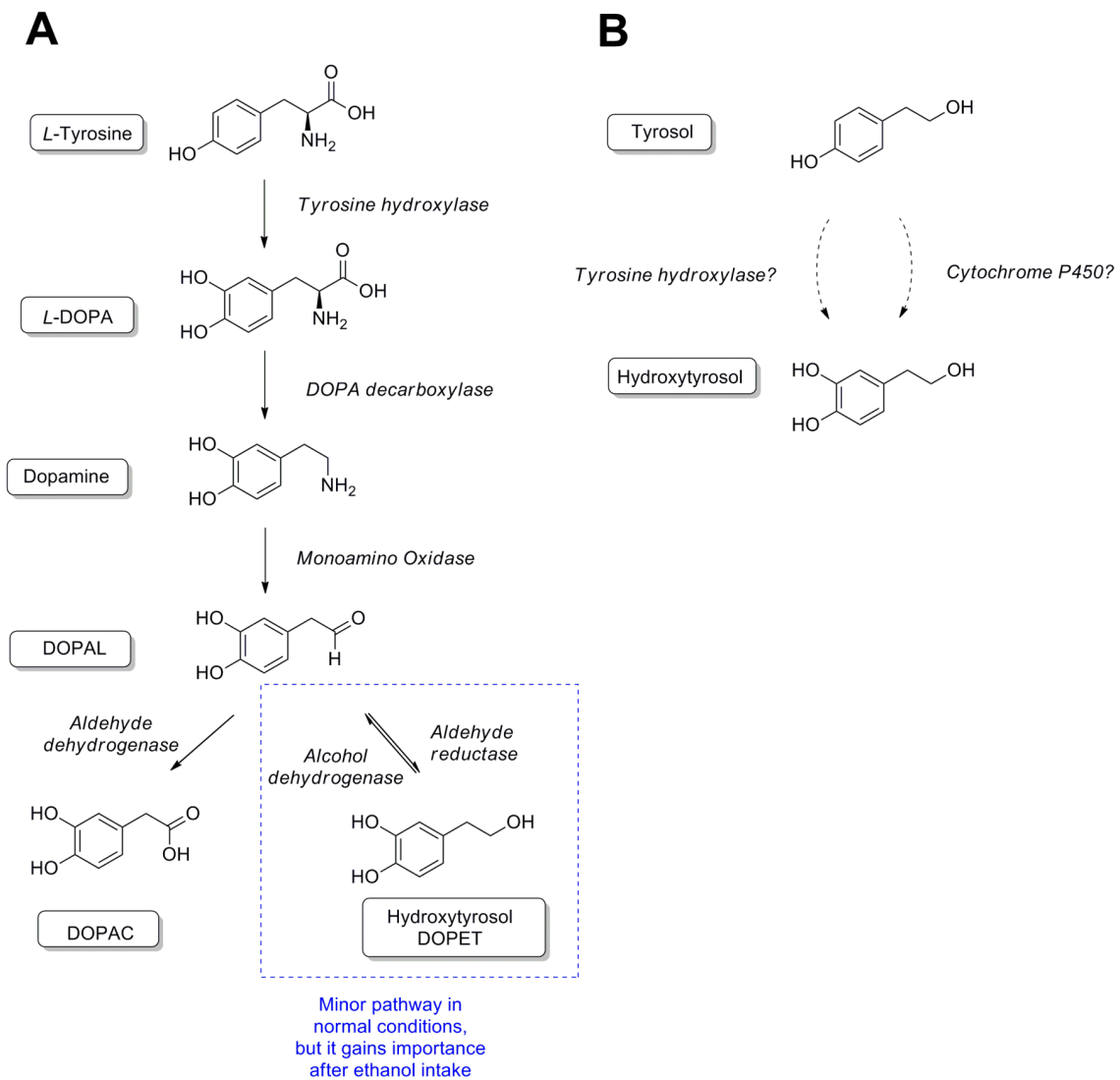
677 Tyndale, R. F., Droll, K. P., & Sellers, E. M. (1997). Genetically deficient CYP2D6  
678 metabolism provides protection against oral opiate dependence.  
679 *Pharmacogenetics*, 7 (5), 375-379.

680 Tyndale, R. F., Inaba, T., & Kalow, W. (1989). Evidence in humans for variant  
681 allozymes of the nondeficient sparteine/debrisoquine monooxygenase (P450IID  
682 1) in vitro. *Drug Metabolism and Disposition*, 17 (3), 334-340.

683 Wassenaar, C. A., Zhou, Q., & Tyndale, R. F. (2015). CYP2A6 genotyping methods  
684 and strategies using real-time and end point PCR platforms. *Pharmacogenomics,*  
685 *17 (2)*, 147-162.

686 Yokoi, T., & Kamataki, T. (1998). Genetic polymorphism of drug metabolizing  
687 enzymes: new mutations in CYP2D6 and CYP2A6 genes in Japanese.  
688 *Pharmaceutical Research*, 15 (4), 517-524.

689 Zhang, W., Kilicarslan, T., Tyndale, R. F., & Sellers, E. M. (2001). Evaluation of  
690 methoxsalen, tranylcypromine, and tryptamine as specific and selective  
691 CYP2A6 inhibitors in vitro. *Drug Metabolism and Disposition*, 29 (6), 897-902.  
692  
693

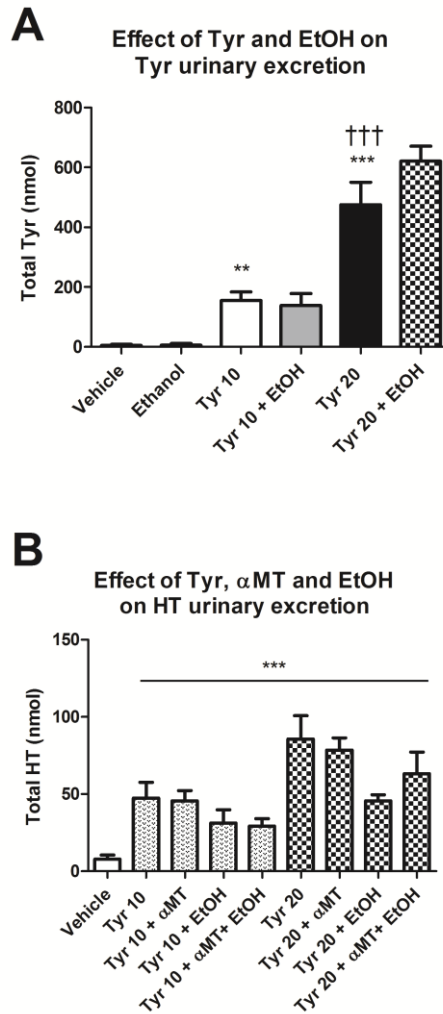


695

696 **Figure 1**

697 **A**, Dopamine biosynthesis and oxidative metabolism. Hydroxytyrosol is produced as a  
 698 metabolite of dopamine ( DOPET) and this formation is increased after ethanol intake in  
 699 humans. **B**, Schematic representation of the two hypotheses considered: (i) tyrosine  
 700 hydroxylase converts tyrosol into hydroxytyrosol as it converts tyrosine to *L*-DOPA; (ii)  
 701 cytochrome P450 is responsible for the hydroxylation.

702



703

704 **Figure 2**

705 Total tyrosol (Tyr) and hydroxytyrosol (HT) urinary excretion (0-4 h) in rats. **A**, Tyr  
 706 urinary recoveries following Tyr administration with and without ethanol (0.5 g/kg); **B**,  
 707 HT urinary excretion following the administration of Tyr (10 and 20 mg/kg),  $\alpha$ -methyl-  
 708 *L*-tyrosine ( $\alpha$ MT; 50 mg/kg) and ethanol (0.5 g/kg).

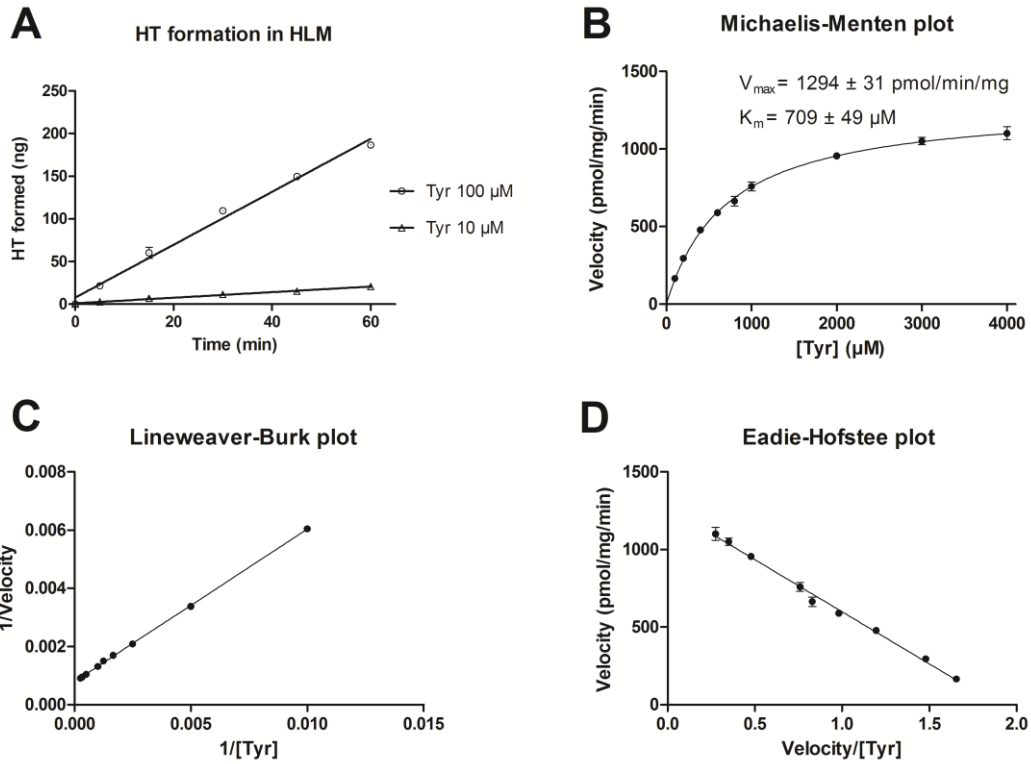
709 Data expressed as mean  $\pm$  SEM.

710 \*\* $P < 0.005$ , versus vehicle; \*\*\* $P < 0.001$ , versus vehicle; †††  $P < 0.05$ , versus Tyr 10  
 711 mg/kg

712  $\alpha$ MT:  $\alpha$ -methyl-*L*-tyrosine; EtOH: Ethanol; Tyr 10: Tyrosol 10 mg/kg; Tyr 20: Tyrosol

713 20 mg/kg





715

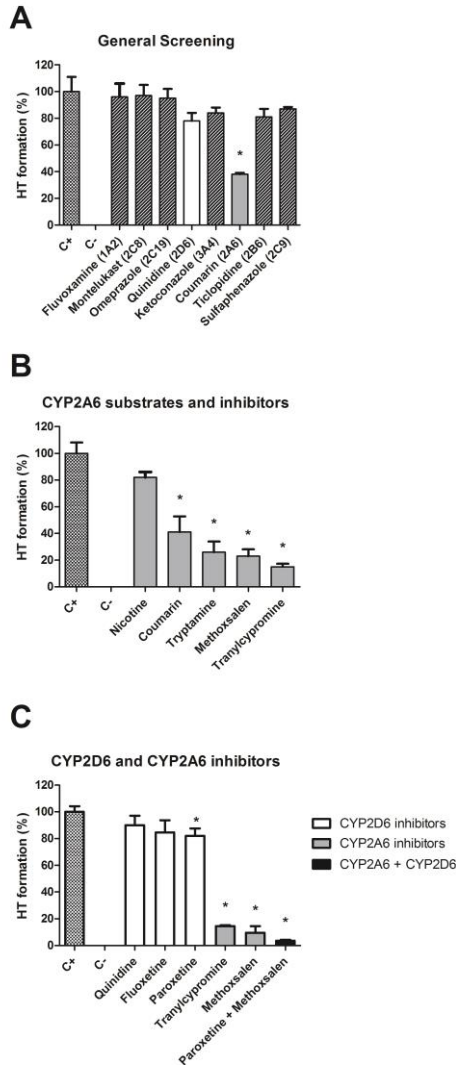
716 **Figure 3**

717 Hydroxytyrosol (HT) formation from tyrosol in human liver microsomes (HLM). **A**,

718 Time- and dose-dependent formation; **B**, Michaelis-Menten plot; **C**, Lineweaver-Burk

719 plot; **D**, Eadie-Hofstee plot.

720



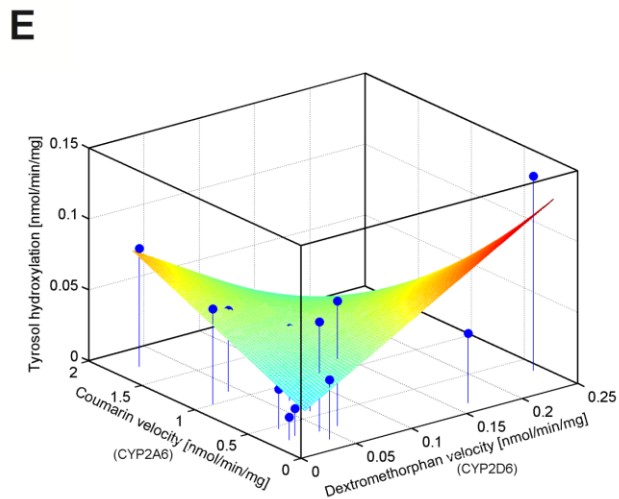
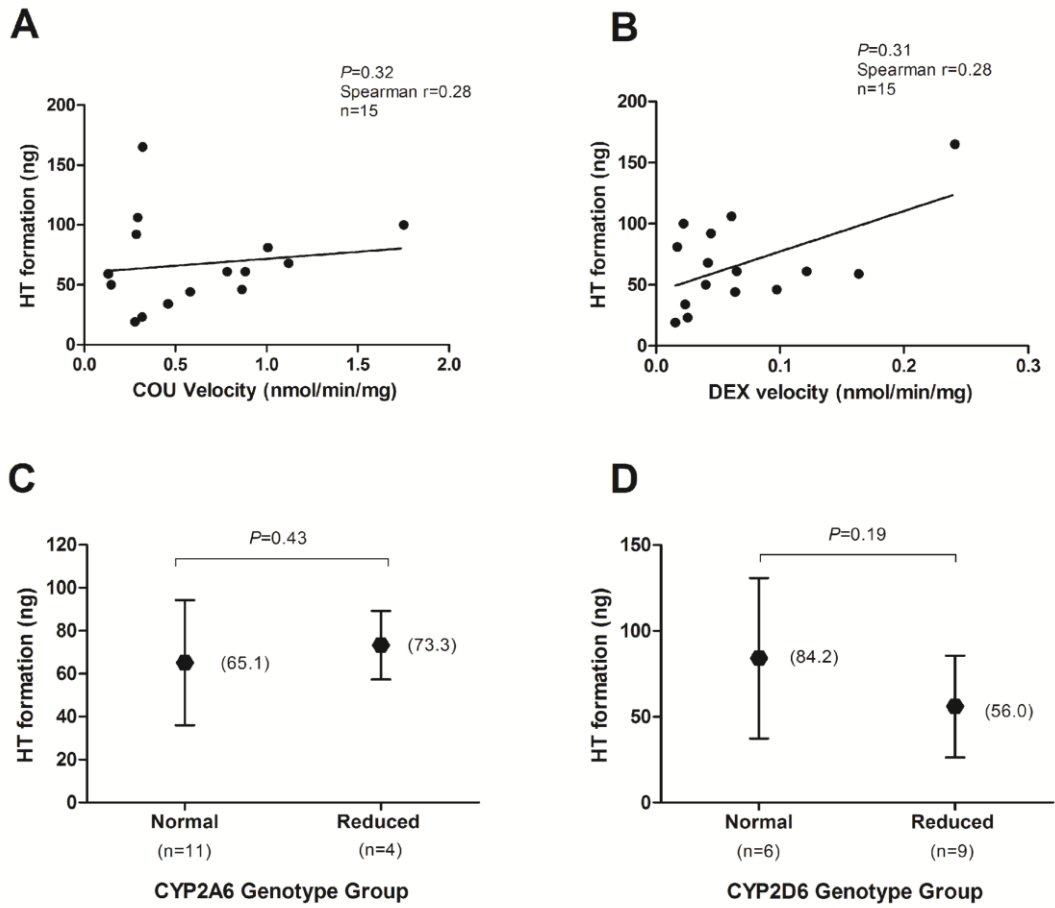
721

722 **Figure 4**

723 Inhibitory effect of cytochrome P450 (CYP) isoenzyme specific inhibitors on the  
 724 formation of hydroxytyrosol (HT) from tyrosol; **A**, Primary screening including  
 725 selective inhibitors of 8 different isoenzymes; **B**, Confirmatory incubations using  
 726 nicotine as a CYP2A6 substrate and selective CYP2A6 inhibitors (tryptamine,  
 727 methoxsalen and tranlycypromine); **C**, Additional experiments to evaluate the potential  
 728 effect of different inhibitors of CYP2A6 and CYP2D6. In this case, microsomes were  
 729 pre-incubated with inhibitors for 30 min.

730 Values are given as mean  $\pm$  standard deviation of two independent experiments.

731 \*  $P < 0.05$ .



732

733

734 **Figure 5**

735 **A.** Correlation between hydroxytyrosol (HT) formation and CYP2A6 activity

736 (determined using the metabolism velocity of coumarin to 7-hydroxycoumarin).

737 **B.** Correlation between HT formation and CYP2D6 activity (determined using the

738 metabolism velocity of dextromethorphan to dextrorphan). *P* and *r* values are based on

739 Spearman correlation test.

740 **C.** Association between *CYP2A6* genotype and HT formation (ng). Normal

741 metabolizers are those with *\*1/\*1*, *\*1/\*1X2*, and *\*14/\*14* *CYP2A6* genotypes. Reduced

742 metabolizers are those with *CYP2A6* *\*1/\*2* and *\*1/\*12* genotypes.

743 **D.** Association between *CYP2D6* genotype and HT formation (ng). Normal

744 metabolizers are those with *\*1/\*1* *CYP2D6* genotype. Reduced metabolizers are those

745 with *CYP2D6* *\*1/\*3*, *\*1/\*4*, and *\*10/\*10* genotypes. *P* values are based on Mann-

746 Whitney tests.

747 **E.** Multivariate correlation analysis of sample-to-sample variation (*n* = 15) in tyrosol-3-

748 hydroxylation with CYP2D6 and CYP2A6 activities.